THE JOURNAL OF PHYSICAL CHEMISTRY Letters

pubs.acs.org/JPCL

Synchronization of Chemical Micro-oscillators

Masahiro Toiya,[†,§,∥] Hector O. González-Ochoa,[‡,∥] Vladimir K. Vanag,[†] Seth Fraden,[‡] and Irving R. Epstein*[,†]

[†]Department of Chemistry, Brandeis University, Waltham, Massachusetts 02454, [‡]Department of Physics, Brandeis University, Waltham, Massachusetts 02454, and [§]CCS Inc., Burlington, Massachusetts 01803

ABSTRACT Many phenomena of biological, physical, and chemical importance involve synchronization of oscillatory elements. We explore here, in several geometries, the behavior of diffusively coupled, nanoliter volume, aqueous drops separated by oil gaps and containing the reactants of the oscillatory Belousov–Zhabotinsky (BZ) reaction. A variety of synchronous regimes are found, including in- and antiphase oscillations, stationary Turing patterns, and more complex combinations of stationary and oscillatory BZ drops, including three-phase patterns. A model consisting of ordinary differential equations based on a simplified description of the BZ chemistry and diffusion of messenger (primarily inhibitory) species qualitatively reproduces most of the experimental results.

SECTION Kinetics, Spectroscopy

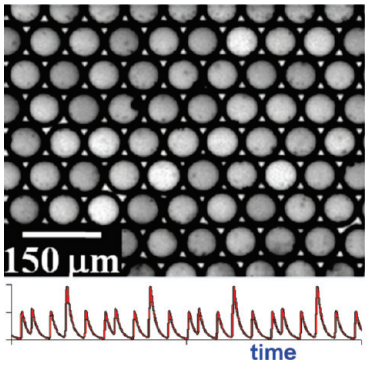

Studies of synchronized oscillators have generated significant insights into a diverse array of physical, chemical, and biological phenomena since the first known efforts by Huygens in the seventeenth century.[1] In biology, coupled oscillator approaches have been applied, for example, in modeling the growth of slime molds,[2] bimanual coordination of vertebrates,[3−5] and in much more complex simulations of the human brain.[6] The coupling can be local or global (e.g., all-to-all) or a combination,[7,8] as well as attractive (excitatory) or repulsive (inhibitory). Global inhibitory coupling in chemical or electrochemical oscillatory systems led to the discovery of such new patterns as oscillatory or chaotic clusters.[9,10] Global excitatory coupling usually results in system-wide in-phase synchronization (above a critical value of the coupling strength).[11] When the coupling is purely excitatory or when excitatory coupling is dominant,[12,13] a system typically has two states: asynchronous, in which the oscillators have random phases, and synchronous, when all oscillators are in-phase with one another. Time delays associated with the coupling can complicate this simplified picture.

Local inhibitory coupling has been much less investigated experimentally, though it is found in many important cases. Examples of inhibitory coupling include interneuron communication in the brain[6] and coupled semiconductor lasers.[14] Several theoretical works suggest that inhibitory coupling should produce many different synchronous regimes and multistability between them.[15−19] Recently, we developed an experimental system consisting of a linear array of small (50−300 μm in diameter) identical water droplets separated by oil gaps.[20] Each drop contains the reactants of the oscillatory Belousov–Zhabotinsky (BZ) reaction:[21,22] malonic acid (MA), bromate, sulfuric acid, ferroin (catalyst), and a small amount of $Ru(bpy)_3$, which serves both as a cocatalyst and to make the BZ reaction photosensitive. Droplets are diffusively coupled through the inhibitor, Br_2, which preferentially dissolves in the oil gaps. We observed antiphase synchronization and stationary Turing patterns in this system.[20]

In this letter we report new synchronized patterns observed in two-dimensional (2D) arrays of oscillatory BZ microdrops, as well as novel, more complex patterns found in linear (1D) configurations and in arrays of partially stacked ("1.5D") drops. Thus we experimentally confirm that inhibitory coupling is able to produce a rich variety of patterns.

In the 1D configuration, the most stable behavior is the previously reported antiphase oscillation,[20] in which each drop is 180° out of phase with its neighbors. If we synchronize the drops initially with a flash of light and block communication between drops by adding a bromine scavenger to the oil between drops (see Supporting Information, Methods), then we initially observe in-phase synchronization, but, because there are small differences in frequency between the drops, this regime demonstrates a slow phase drift that soon destroys the synchrony. If no scavenger is employed, the drops remain in phase for tens of oscillations, indicating active in-phase synchronization (see Supporting Information, Figure S1). Our simulations show, however, that in-phase synchronization with inhibitory coupling has a much smaller basin of attraction than antiphase synchronization. Experimentally, delaying the phase of a single drop in a synchronized in-phase 1D arrangement with a focused laser beam initiates a transition to an antiphase pattern that propagates out from the delayed drop. Indeed, a quite precise in-phase initial condition among all drops is necessary to produce in-phase synchronization.

In the 1.5D experiments, when the drop diameter lies between $0.5d$ and d, where d is the inner diameter of the glass

Received Date: February 19, 2010
Accepted Date: March 18, 2010
Published on Web Date: March 26, 2010

DOI: 10.1021/jz100238u | J. Phys. Chem. Lett. 2010, 1, 1241–1246

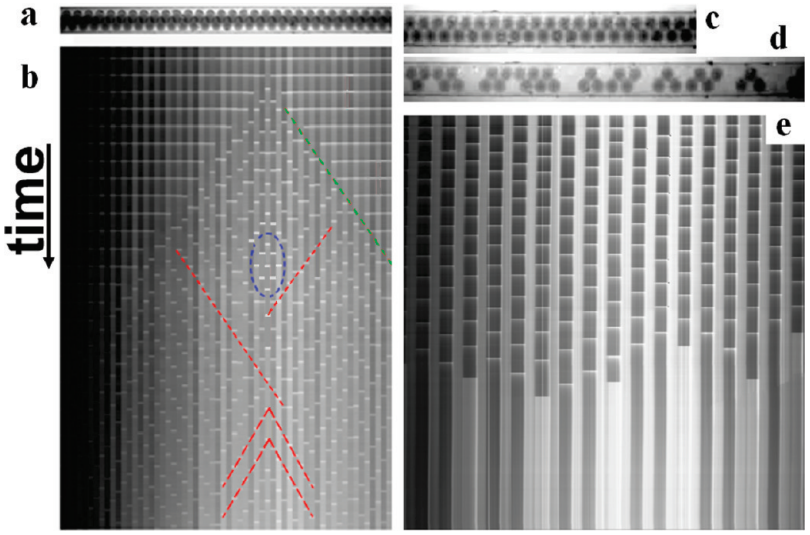

Figure 1. Snapshots (a,c,d) and space-time plots (b), (e, 1D) of patterns emerging from initially in-phase arrays of partially stacked (1.5D) BZ drops in a 150 μm ID capillary. In frames b and e, spikes of oxidation of ferroin are seen as short horizontal light lines (flashes) across BZ-drops. In frames a and b, horizontal length of the frame is 3.8 mm; total time shown in b is 3900 s. In frames c, d, and e, horizontal lengths are 1.6, 2.2, and 4.6 mm, respectively. Total time shown in e is 12 000 s. Initial concentrations of reactants: $[H_2SO_4]$ = 0.08 M, $[NaBrO_3]$ = 0.288 M, [MA] = 0.64 M (a, b), 0.040 M (c−e), [NaBr] = 10 mM, [ferroin] = 3 mM, and $[Ru(bpy)_3]$ = 0.4 mM (bpy = bipyridine).

capillary, the drops self-organize to form a zigzag structure (Figure 1a). This geometry, in which each drop has four neighbors, two near and two more distant, produces a wealth of new stable patterns, some of which are shown in Figures 1 and 2. The space−time plots consist of the intensity taken along a horizontal line through the center of the capillary as a function of time. In Figure 1b we follow the evolution of 60 drops in one very complex regime, in which all the drops oscillate. Initially, all drops are in-phase, but in the second cycle shown, drop 38 (numbering starts from the left) experiences a delay in flashing. This phase shift cascades to the neighboring drops, generating a switching wave shown by the green dotted lines. The velocity of this wave is about 0.8 μm/s, approximately equal to the linear size of a drop divided by the period of oscillation. Note, however, that the oscillation period can vary significantly depending on the synchronous regime. For example, the period of the initial in-phase regime is much shorter than that of the final staggered pattern. The same behavior emerges in the simulations.

Looking carefully at Figure 1b, we see that the drops near drop 38 oscillate 180° out-of-phase with their neighbors. A typical stretch of out-of-phase behavior is marked by the blue oval. Other sets of neighboring drops assume phase differences close to ±120°, as highlighted by red dashed lines in Figure 1b. There are also several pairs of neighboring drops that oscillate in-phase from time to time. A simpler behavior in 1.5D, stationary Turing patterns found at a lower MA concentration, is illustrated in Figure 1c,d,e. In the experiment shown in Figure 1c,d, all drops initially oscillate in-phase after a brief synchronizing illumination (Figure 1c). Soon, each drop ceases to oscillate and reaches a stationary reduced or oxidized state, forming the Turing structure (Figure 1d). The characteristic length of this pattern is several drops, suggesting that the Turing wavelength can be larger, perhaps much larger, than the distance between neighboring drops. The dynamics of an array of drops in a 1D chain that ultimately reaches a stationary and more regular Turing pattern obtained in another experiment is shown in Figure 1e. Here, the characteristic length of the pattern comprises exactly two drops in a reduced state and one drop in an oxidized state. Note that before the system reaches the stationary Turing regime, the drops oscillate antiphase.

Figure 2 demonstrates a novel pattern found in the 1.5D geometry, where all drops in one row (see Figure 2a,d) are stationary, while drops in the other row oscillate antiphase. Figure 2b shows the initial stage of these oscillations, and Figure 2c shows the final stable regime. These drops were not initially synchronized, as no $Ru(bpy)_3$ was added to this system, so the drops begin to oscillate with random phases (Figure 2b). A schematic representation of the pattern behavior is shown in Figure 2d: drops in the bottom row (represented as blue or red) oscillate antiphase, while drops in the upper row remain in a stationary reduced state (gray). The spatial period of this pattern consists of four drops. This pattern is neither a Turing pattern nor a simple antiphase oscillatory pattern. It is difficult to identify an analogous behavior in the homogeneous spatially extended reaction−diffusion system, although if we equate stationary drops to nodes, then this pattern might be thought of as a discrete analog of a standing wave. Another possible analogy is to the oscillatory out-of-phase Turing patterns found recently.[23,24]

In 2D geometry, the drops, when packed at high density, spontaneously form a hexagonal array. The regime consisting of antiphase oscillation between all neighboring pairs, which is extremely stable in the 1D geometry, is impossible in a hexagonal 2D geometry. A similar, symmetry-generated situation arises in an analogous Hamiltonian system: the 2D antiferromagnetic XY model.[25,26] To resolve this geometrical constraint, our drops respond in different ways. Figure 3a shows a pattern, denoted "π-S", in which stationary drops

DOI: 10.1021/jz100238u | J. Phys. Chem. Lett. 2010, 1, 1241–1246

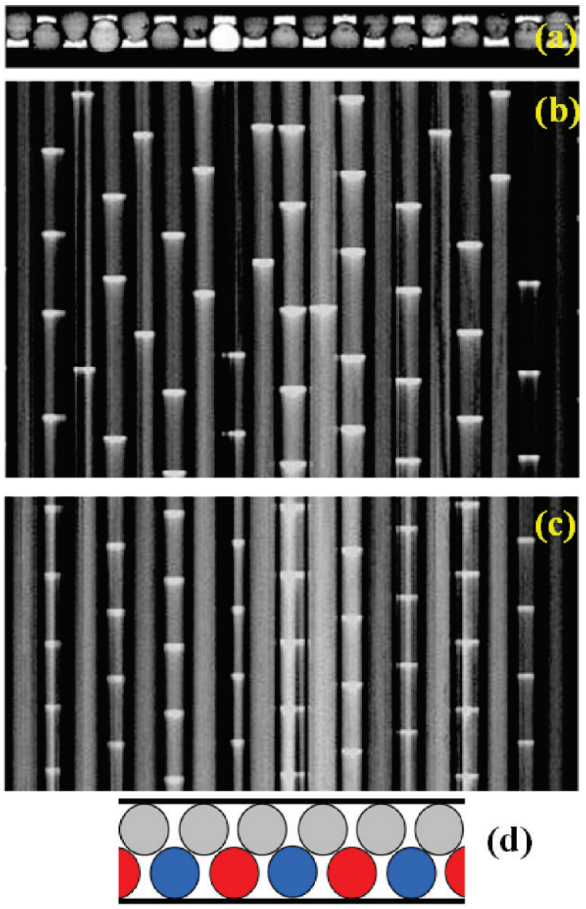

Figure 2. Pattern consisting of stationary and antiphase oscillatory BZ drops in 1.5D geometry. (a) Snapshot of capillary with BZ drops; (b,c) space−time plots (time-axis is vertical) for (b) early times during transient period and (c) later, after the stationary regime is established; (d) schematic representation of the pattern. Initial concentrations of BZ reagents are as in Figure 1 with [MA] = 0.64 M, except [$Ru(bpy)_3$] = 0. Drop size is 65 μm. Oscillation period is 177 s. Length of frames is 1.044 mm. Times shown in frames b and c are 1068 and 798 s, respectively.

(black) surrounded by six oscillating antiphase drops form a larger hexagonal pattern. Figure 3b shows this pattern schematically, with stationary drops in gray, and blue and red drops oscillating out of phase by nearly 180°. As a result, drop 10 (or drops 2, 4, 7, 13, 16, 18, etc.) in Figure 3b is exposed to inhibitory bromine signals twice as often as any of the red−blue pairs. This inhibition is apparently sufficient to prevent it from oscillating, pushing it into a stationary reduced state. This 2D pattern bears similarities to the mixed stationary−oscillatory 1.5D pattern shown in Figure 2; however, the spatial period of the pattern in Figure 3 taken along any of the three hexagonal axes consists of three drops. Figure 3c,d shows space−time plots for selected drops, confirming the antiphase behavior of neighboring drops.

A second configuration for drops in 2D, denoted "$2\pi/3$," is shown in Figure 4, where the neighboring drops oscillate with a phase shift close to 120°, corresponding to the ground state of the 2D antiferromagnetic XY model.[25,26] A snapshot of the system is shown in Figure 4e, with the outlined region

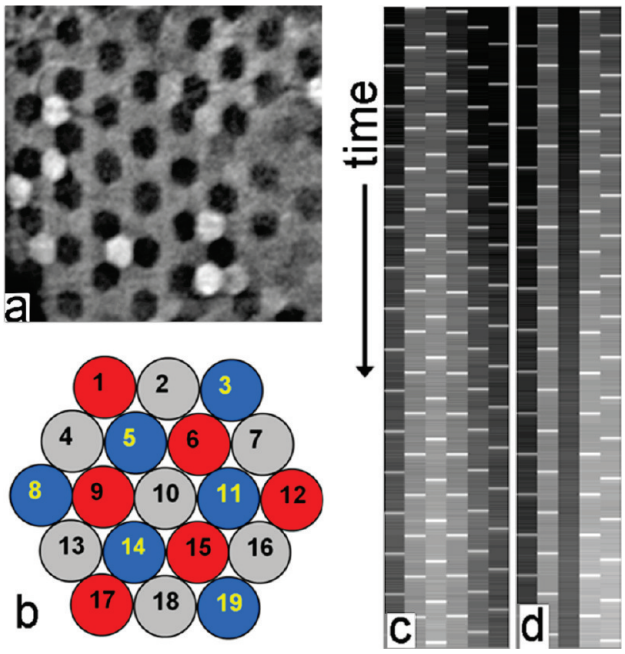

Figure 3. Stationary and antiphase oscillatory BZ drops in 2D. (a) Hexagonally packed drops forming a larger hexagon with each stationary drop (black) surrounded by six oscillatory drops. Imaged area is 0.7 × 0.7 mm. (b) Schematic representation of the pattern (stationary drops in gray). (c,d) Space−time plots (duration 2800 s) of drops 6, 11, 15, 14, 9, and 5 (c) and drops 1, 5, 10, 15, and 19 (d). Concentrations of BZ reagents are as in Figure 1.

of interest magnified in Figure 4f. Frames a−d are snapshots of the region centered around drop 1 in Figure 4f taken after the stationary behavior has been reached. The interval between snapshots is about 73 s, i.e., 1/3 of the single drop oscillation period of 220 s. Drops 2, 4, and 6 oxidize in-phase in frame a, followed by in-phase oxidation of drop 1 and its symmetrically equivalent counterparts (b), and finally drops 3, 5, and 7 (c). The cycle starts again in frame (d). Figure 4g shows a staggered space−time plot of drops 1−7, marked in (f). This regime resembles the portions of Figure 1b with phase shift ≅ 120° between neighboring drops. The most important difference between the conditions that result in the two patterns illustrated in Figure 3 (π-S) and Figure 4 ($2\pi/3$) is that π-S patterns are obtained at stronger coupling, which we can characterize by the dimensionless ratio $D/(kL^2)$. Here D is the effective diffusion coefficient of the inhibitor (bromine), k is the effective (first-order) rate constant for the consumption of the inhibitor, and L is the distance between drops. There are at least two ways to increase the coupling strength: (*i*) by decreasing the size of the water droplets or (*ii*) by decreasing the length of the oil gap between droplets. We explored both methods (to decrease the oil gap, we decreased the amount of oil in the emulsion). With either method, an increase in coupling strength (e.g., by decreasing the droplet diameter from 120 to 90 μm) leads to a transition from the $2\pi/3$ to the π-S pattern. More generally, stronger coupling results in a higher proportion of stationary droplets, a result found in both the experiments and the simulations. The simulations

DOI: 10.1021/jz100238u | J. Phys. Chem. Lett. 2010, 1, 1241–1246

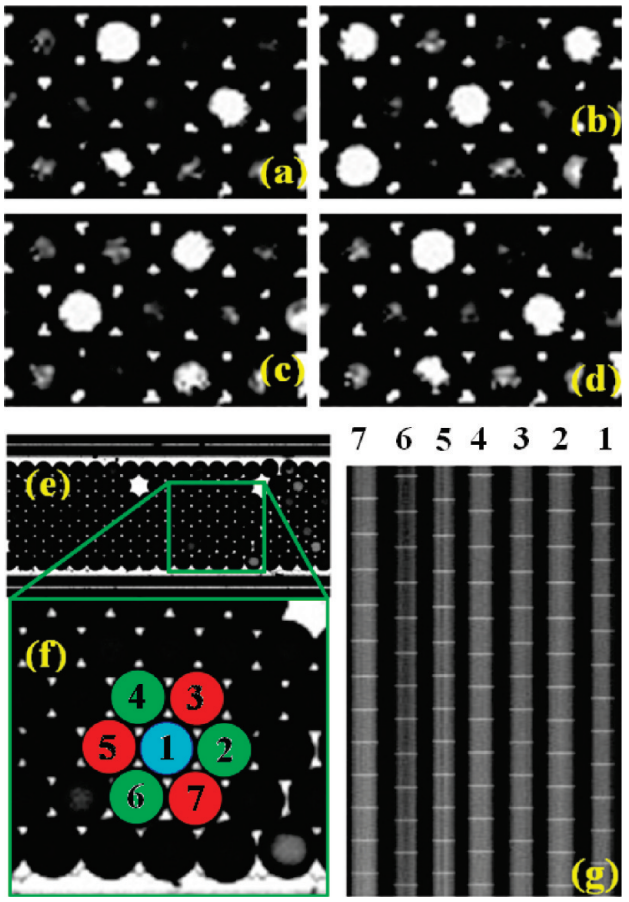

Figure 4. Three-phase oscillatory clusters in 2D. Drop diameter is 128 μm. Initial concentrations: $[H_2SO_4]$ = 0.08 M, $[NaBrO_3]$ = 0.29 M, [MA] = 0.64 M, [Ferroin] = 3 mM, [NaBr] = 0.01 M, and $[Ru(bpy)_3]$ = 1.2 mM. Snapshots a−d are taken at t = 0, $T/3$, $2T/3$, and T, where $T \cong 231$ s. Snapshot e and its enlargement (f) show a 2D configuration of BZ drops. (g) Space−time plot for drops 1−7 shown in snapshot f; dimensions are 896 μm horizontal and 2877 s vertical. Period of oscillations for each drop in the space−time plot is the same as T in snapshots a−d.

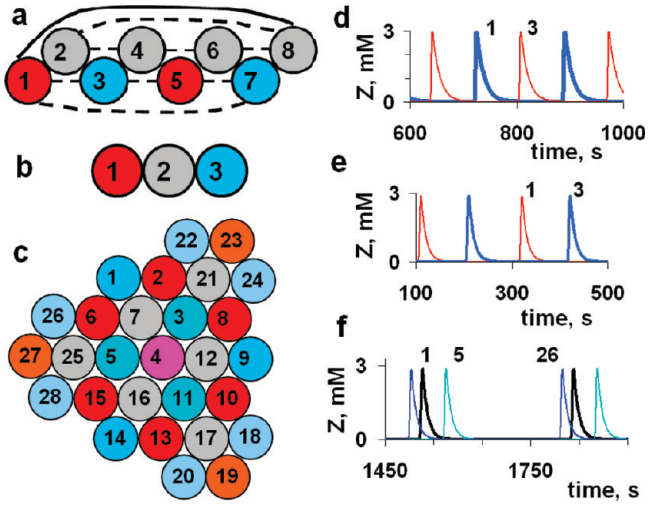

Figure 5. Simulations. (a,d) Eight identical coupled BZ drops for 1.5 D configuration. (a) Gray drops are stationary. Drops 1 and 5 oscillate in-phase, drops 3 and 7 also oscillate in-phase but antiphase to drops 1 and 5. (d) Oscillations of drops 1 and 3, T = 165.5 s, z is the oxidized form of the catalyst. Chemical parameters: $h = [H^+]$ = 0.2 M, $a = [BrO_3^-]$ = 0.3 M, m = [MA] = 0.5 M, c_0 (total concentration of the catalyst) = 0.003 M. Coupling parameters: k_f (coupling strength between close droplets like 1 and 2) = 1 s^{-1}, $1/k_b$ (associated with time delay in coupling) = $P_B/\rho_V k_f$, P_B (partition coefficient for Br_2 between water and oil) = 2.5, ρ_V (volume ratio of water drops and oil gaps) = 10, k_{fd} (coupling strength between distant droplets like 1 and 3 in frame a) = $k_f/10$, ρ_{V2} = 2, $k_{bd} = \rho_{V2} k_{fd}/P_B$, $k_O = k_{fr} = 0$. (b,e) The minimum number (three) of drops simulating the pattern in Figure 3. The gray drop is stationary. Drops 1 and 3 oscillate antiphase, as shown in frame e. Parameters: h = 0.16 M, a = 0.3 M, m = 0.65 M, k_f = 1 s^{-1}, P_B = 2.5, ρ_{V2} = 10. (c,f) Twenty-eight identical hexagonally packed BZ drops. (c) Gray drops (7, 21, 12, 25, 16, and 17) are in the oxidized SS (oscillates with very small amplitude). Reddish drops oscillate almost in-phase. Bluish drops also oscillate almost in-phase and antiphase to reddish drops. (e) phase shift between three types (with slightly different environments) of bluish drops (1, 5, and 26). Parameters: as in (b,e) except k_f = 0.4 s^{-1}. Other constants used in the FKN model S1−S12 are specified in the caption for Figure 3S in the Supporting Information.

further suggest that, in the limit of very strong coupling, a limit we have achieved in the 1D but not in the 2D experiments, all droplets become stationary, resulting in Turing patterns. At intermediate coupling strengths, the slightly different initial conditions may also contribute to the selection of different final patterns by our system. In both cases, we have patterns consisting of three groups of droplets having either different phases or different dynamical behavior (stationary or oscillatory drops).

To better understand our experimental results, we carried out computer simulations on a simplified model of our system S1−S12, described in the Supporting Information, Modeling. Because, even at this level of simplification, modeling large arrays of drops is computationally taxing, we explored mainly configurations consisting of small numbers of drops to see whether the key features of our 1D, 1.5D, and 2D systems would emerge.

Typical results of simulations are shown in Figure 5. The regime seen in Figure 2 with stationary and antiphase oscillatory BZ drops is reproduced in Figure 5a,d for an eight-drop array in the 1.5D configuration. Stationary Turing patterns resembling the experimental patterns shown in Figure 1d,e are presented in the Supporting Information, Results (Figure S3). Such Turing patterns are obtained with stronger inhibitory coupling (through bromine) and/or at smaller concentrations of MA, as in the experiments. Note that a decrease in [MA] leads to higher $[Br_2]$ in the drops and the intervening oil and consequently gives stronger inhibitory coupling.

The 2D pattern shown in Figure 3 can be simulated with an array of three linearly coupled drops in 1D shown in Figure 5b,e (where the central drop is nearly stationary and the two end drops oscillate antiphase, over a broad range of concentrations) and several configurations of hexagonally packed drops shown in Figure 5c. For example, if we take only drops 1−7 as labeled in Figure 5c, drops 1−12, 1−16, 1−20, or 1−24, we obtain patterns as in Figure 3. However, if the number of drops in our cluster is small (less than about 20), the final pattern is very sensitive to the addition or removal of a single droplet. A cluster of 28 drops (shown in Figure 5c) is much less sensitive to this procedure. A number of

DOI: 10.1021/jz100238u | J. Phys. Chem. Lett. 2010, 1, 1241–1246

questions about the sensitivity of the pattern to the number of droplets, the coupling strength, the symmetry of the droplet configuration, and the initial conditions remain. Note that droplets that oscillate "in-phase," like the reddish or bluish droplets in Figure 5c, have a slight phase shift, as shown in Figure 5f. An analogous phase shift can be seen in all our experimental results. The origin of this shift in the simulations is the different number of neighbors for boundary and "inner" droplets.

The three-phase oscillatory patterns shown in Figure 4 can be simulated with just three circularly coupled BZ drops plus three oil drops (like drops 1, 2, and 7 in Figure 5c, for example; see also Supporting Information, Results, Figure S4). Curiously, the three-phase pattern of Figure 3 cannot be modeled with three circularly coupled drops. Both of the two three-phase patterns in 2D, π-S and $2\pi/3$, are found in a cluster of six identical drops connected in 3D to form an octahedron (Supporting Information, Results, Figure S5). This unique configuration allows us to have periodic boundary conditions, an even number of neighbors (4 vs 6 in hexagons), and a total number of drops divisible by 3 (the spatial period for these two patterns). Simulations reveal that an increase in coupling strength leads to a transition from $2\pi/3$ to π-S patterns, just as we observe in our experiments. However, there is no clear physical correspondence between the experimental configuration of hexagonally packed drops and the simulations on 3D octahedrons.

In our simulations, we used the well-known FKN mechanism for the BZ reaction,[27] in which $BrO_2^{\bullet}$ radical serves as an excitatory messenger between droplets, and Br_2 acts as an inhibitory messenger. Excluding $BrO_2^{\bullet}$ as a messenger in the model causes almost no change in the calculated patterns, which suggests that this species plays practically no role in the coupling.

The formation of two-phase and three-phase structures, i.e., sets of drops that oscillate with a common phase (or are stationary) in our system, may be viewed as a generalization of the chemical quorum sensing recently reported[13] in sets of particles loaded with catalyst and immersed in a BZ solution. Here, too, the individual drops behave independently until brought together so that their density (or coupling strength) exceeds a critical value. They then begin to exhibit more complex dynamical behavior, in our case antiphase and three-phase patterns as well as the in-phase oscillation observed in the particle experiments. Our oscillatory structures also resemble the clusters observed in experiments on globally coupled electrochemical oscillators.[10] The larger the coupling strength, the larger the number of different synchronous groups (up to the limit of Turing patterns). Therefore in addition to the "quorum sensing", our system exhibits a primitive kind of "differentiation".

Since the coupling of our oscillatory BZ drops is primarily inhibitory, and they can form stationary Turing-like patterns (if the coupling is strong enough), this system can be viewed as a discrete manifestation of the Turing−Hopf interaction that generates many interesting patterns in continuous reaction-diffusion systems, such as oscillatory in-phase and antiphase Turing patterns (the latter is analogous to our antiphase regime).[23,24]

All configurations that we have studied computationally demonstrate multiple synchronous regimes, i.e., regimes in which each drop has the same total period (though possibly with different numbers of maxima during this period). We expect to find some of these regimes in further experiments on our system of coupled BZ droplets, which mimics diffusive inhibitory coupling among biological objects, a situation that is ubiquitous in nature.

SUPPORTING INFORMATION AVAILABLE

Methods, modeling, and results as Figures S1−S5. This material is available free of charge via the Internet at http://pubs.acs.org.

AUTHOR INFORMATION

Corresponding Author:

*To whom correspondence should be addressed. E-mail: epstein@brandeis.edu.

Author Contributions:

‖ These authors contributed equally to this work.

ACKNOWLEDGMENT

This work was supported by the National Science Foundation (CHE-0615507 and MRSEC DMR-0820492) and by the Defense Advanced Research Projects Agency. M.T. and I.R.E. thank Milos Dolnik and the late Anatol Zhabotinsky for helpful comments and suggestions. We thank CCS Inc. for providing the LED illuminator used in some of the experiments in this work.

REFERENCES

(1) Strogatz, S. H. *SYNC: The Emerging Science of Spontaneous Order*; Hyperion: New York, 2003.
(2) Saigusa, T.; Tero, A.; Nakagaki, T.; Kuramoto, Y. Amoebae Anticipate Periodic Events. *Phys. Rev. Lett.* **2008,** *100*, 018101.
(3) Grossberg, S.; Pribe, C.; Cohen, M. A. Neural Control of Interlimb Oscillations 0.1. Human Bimanual Coordination. *Biol. Cybern.* **1997,** *77*, 131–140.
(4) Butt, S. J. B.; Lebret, J. M.; Kiehn, O. Organization of Left−Right Coordination in the Mammalian Locomotor Network. *Brain Res. Rev.* **2002,** *40*, 107–117.
(5) Uematsu, K.; Baba, Y.; Kake, Y.; Ikenaga, T.; Moon, S. J.; Yoshida, M. Central Mechanisms Underlying Fish Swimming. *Brain Behav. Evol.* **2007,** *69*, 142–150.
(6) Izhikevich, E. M. *Dynamical Systems in Neuroscience: The Geometry of Excitability and Bursting*; MIT Press: Cambridge, MA, 2007.
(7) Pikovsky, A.; Rosenblum, M.; Kurths, J. *Synchronization. A Universal Concept in Nonlinear Sciences*; University Press: Cambridge, U.K., 2001.
(8) Abrams, D. M.; Strogatz, S. H. Chimera States for Coupled Oscillators. *Phys. Rev. Lett.* **2004,** *93*, 174102.
(9) Vanag, V. K.; Yang, L.; Dolnik, M.; Zhabotinsky, A. M.; Epstein, I. R. Oscillatory Cluster Patterns in a Homogeneous Chemical System with Global Feedback. *Nature* **2000,** *406*, 389–391.
(10) Wang, W.; Kiss, I. Z.; Hudson, J. L. Clustering of Arrays of Chaotic Chemical Oscillators by Feedback and Forcing. *Phys. Rev. Lett.* **2001,** *86*, 4954–4957.
(11) Kuramoto, Y. *Chemical Oscillations, Waves, and Turbulence*; Springer: Berlin, 1984.
(12) Okano, T.; Miyakawa, K. Feedback-Controlled Dynamics in a Two-Dimensional Array of Active Elements. *Phys. Rev. E* **2009,** *80*, 026215.

(13) Taylor, A. F.; Tinsley, M. R.; Wang, F.; Huang, Z. Y.; Showalter, K. Dynamical Quorum Sensing and Synchronization in Large Populations of Chemical Oscillators. *Science* **2009,** *323*, 614–617.
(14) Sivaprakasam, S.; Pierce, I.; Rees, P.; Spencer, P. S.; Shore, K. A.; Valle, A. Inverse Synchronization in Semiconductor Laser Diodes. *Phys. Rev. A* **2001,** *64*, 013805.
(15) Bressloff, P. C.; Coombes, S. Dynamics of Strongly Coupled Spiking Neurons. *Neural Comput.* **2000,** *12*, 91–129.
(16) Rabinovich, M. I.; Varona, P.; Selverston, A. I.; Abarbanel, H. D. I. Dynamical Principles in Neuroscience. *Rev. Mod. Phys.* **2006,** *78*, 1213–1265.
(17) Senthilkumar, D. V.; Kurths, J.; Lakshmanan, M. Inverse Synchronizations in Coupled Time-Delay Systems with Inhibitory Coupling. *Chaos* **2009,** *19*, 023107.
(18) Volkov, E. I.; Ullner, E.; Zaikin, A. A.; Kurths, J. Frequency-Dependent Stochastic Resonance in Inhibitory Coupled Excitable Systems. *Phys. Rev. E* **2003,** *68*, 061112.
(19) Volkov, E. I.; Stolyarov, M. N.; Zaikin, A. A.; Kurths, J. Coherence Resonance and Polymodality in Inhibitory Coupled Excitable Oscillators. *Phys. Rev. E* **2003,** *67*, 066202.
(20) Toiya, M.; Vanag, V. K.; Epstein, I. R. Diffusively Coupled Chemical Oscillators in a Microfluidic Assembly. *Angew. Chem., Int. Ed.* **2008,** *47*, 7753–7755.
(21) Belousov, B. P. A Periodic Reaction and Its Mechanism. In *Collection of Short Papers on Radiation Medicine*; Medgiz: Moscow, 1959; pp 145−152.
(22) Zhabotinsky, A. M. Periodic Liquid Phase Reactions. *Proc. Acad. Sci. USSR* **1964,** *157*, 392–395.
(23) Kaminaga, A.; Vanag, V. K.; Epstein, I. R. "Black Spots" in a Surfactant-Rich BZ-AOT Microemulsion System. *J. Chem. Phys.* **2005,** *122*, 174706.
(24) McIlwaine, R.; Vanag, V. K.; Epstein, I. R. Temperature Control of Pattern Formation in the $Ru(bpy)_3^{2+}$-Catalyzed BZ-AOT System. *Phys. Chem. Chem. Phys.* **2009,** *11*, 1581–1587.
(25) Korshunov, S. E. Phase Transitions in Two-Dimensional Systems with Continuous Degeneracy. *Phys.-Usp.* **2006,** *49*, 225–262.
(26) Miyashita, S.; Shiba, H. Nature of the Phase-Transition of the Two-Dimensional Antiferromagnetic Plane Rotator Model on the Triangular Lattice. *J. Phys. Soc. Jpn.* **1984,** *53*, 1145–1154.
(27) Field, R. J.; Körös, E.; Noyes, R. M. Oscillations in Chemical Systems. II. Thorough Analysis of Temporal Oscillation in Bromate−Cerium−Malonic Acid System. *J. Am. Chem. Soc.* **1972,** *94*, 8649–8664.

DOI: 10.1021/jz100238u | *J. Phys. Chem. Lett.* **2010,** *1*, 1241–1246